$\delta^{13}C$ and $\delta^{18}O$ ANALYSES OF CARBONATE CONCRETIONS AND NODULES AND THE EVIDENCE FOR A CRETACEOUS GREENHOUSE

JOSEPH M. BENINATI
ADVISOR: LISA GREER
WASHINGTON AND LEE UNIVERSITY

TABLE OF CONTENTS

ABSTRACT **4**

INTRODUCTION **5**

GEOLOGIC BACKGROUND **7**

TECTONIC SETTING: 7

STRATIGRAPHY AND SEDIMENTOLOGY: 9

CLIMATE: 11

$\Delta^{13}C$ AND $\Delta^{18}O$ STABLE ISOTOPES: 12

METHODS **14**

FIELD SURVEYING AND MEASURED SECTIONS: 14

CONCRETION AND NODULE SAMPLING: 16

X-RAY DIFFRACTION ANALYSES: 17

$\Delta^{13}C$ AND $\Delta^{18}O$ ANALYSES: 18

RESULTS **19**

XRD ANALYSES: 19

STABLE ISOTOPE ANALYSES: 21

DISCUSSION **25**

CONCLUSIONS **27**

ACKNOWLEDGEMENTS **28**

WORKS CITED **29**

LIST OF FIGURES AND TABLES

Figure 1: Location Photo of Slope Mountain, North Slope, Alaska.. ..... **5**

Figure 2: Regional Map of the Colville Basin, North Slope, Alaska. **7**

Figure 3: Chronostratigraphic Column of Central North Slope, Alaska.. ..... **9**

Figure 4: Geologic Map of Slope Mountain, North Slope, Alaska, ... **15**

Figure 5: Concretion and Nodule Sample Photos. **16**

Figure 6: X-Ray Diffraction (XRD) Results. **20**

Figure 7: $\delta^{18}O$ plotted against $\delta^{13}C$, including data from McKay et al. (1995), Ufnar et al. (2008), and Suarez et al. (2015) **22**

Figure 8: Average Slope Mountain $\delta^{18}O$ and $\delta^{13}C$ Plotted Stratigraphically **23**

Table 1: Tabular Representation of All Concretion and Nodule $\delta^{18}O$ and $\delta^{13}C$ data.. ..... **24**

Abstract

The Aptian-Albian Torok Formation and Nanushuk Formation rocks of Slope Mountain, also known as the Marmot Syncline, have been interpreted to represent shallow marine, deltaic, and fluvial depositional environments. Middle-Cretaceous climate is most commonly interpreted as a greenhouse-world in which peak temperatures and atmospheric carbon dioxide (CO_2) were as great as any other period in Earth's history. Carbonate nodules and concretions have been found throughout the Nanushuk Formation and Torok Formation. This study investigates the composition of local carbonate concretions and nodules in order to determine whether these samples can be used as paleoclimate proxies. We use x-ray diffraction (XRD) and $\delta^{18}O$ and $\delta^{13}C$ stable isotope analyses to extrapolate Middle-Cretaceous climate conditions. $\delta^{18}O$ results range from 17.40 to 28.10‰ with an average value of 23.66‰. $\delta^{13}C$ results range from -21.73 to 2.20‰ with an average value of -6.19‰. Our $\delta^{18}O$ are in agreement with prior studies that suggest a consistently warm and greenhouse-world Middle-Cretaceous climate. The variance in our $\delta^{13}C$ results may be the result of mixing between terrestrial and marine carbon during Slope Mountain deposition.

Introduction

The sedimentary rocks of Slope Mountain, also known as the Marmot Syncline, have been interpreted to represent shallow marine, deltaic, and fluvial environments of the Torok Formation and Nanushuk Formation (Johnsson and Sokol, 1998). The ages of Slope Mountain sediments are thought to be Aptian-Albian (Johnsson and Sokol, 1998), but these dates were based upon a single sample containing a late Albian palynoflora (Reifenstuhl and Plumb, 1993). The Torok Formation and Nanushuk Formation are widespread across Alaska's North Slope and are generally established to be Aptian-Cenomanian in age (Mull et al., 2003) (Figure 1).

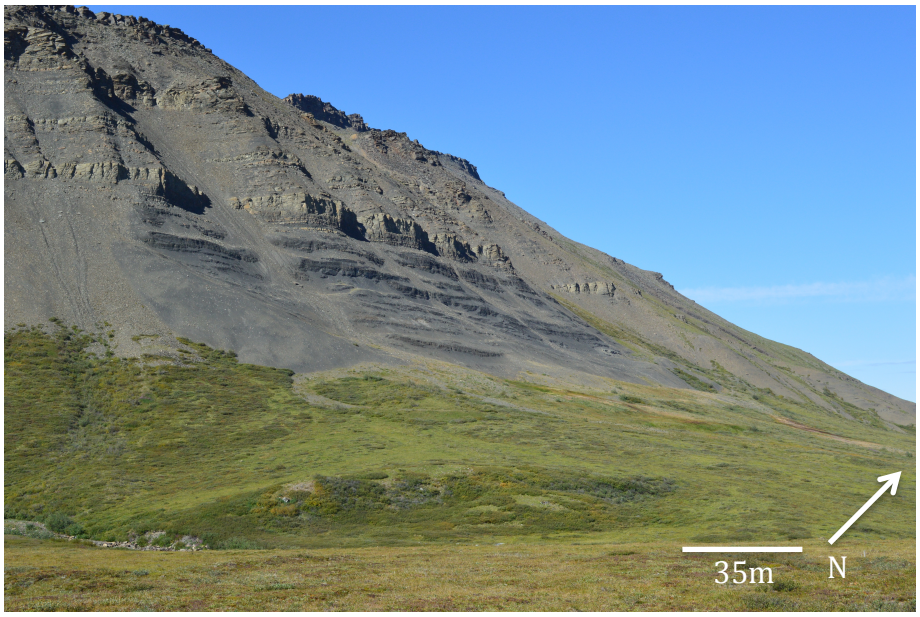

Figure 1: Location photo of Slope Mountain, North Slope, Alaska. The age of Slope Mountain sediments is thought to be Aptian-Albian (Johnsson and Sokol, 1998), but these dates were based upon a single sample containing a late Albian palynoflora (Reifenstuhl and Plumb, 1993). This particular photograph shows SM2.

The middle-Cretaceous climate is most commonly interpreted as a greenhouse-world in which peak temperatures were as great as any other period in Earth's history

(Frakes 1999; Wilson and Norris, 2001; Jenkyns et al., 2004). There is evidence of global CO_2 levels 4 to 5 times those of today, sea-surface temperatures approaching 20 to 21°C, and thermophilic flora and fauna spreading to high-latitudes (Tajika, 1999; Herman and Spicer, 2010). These conditions were likely the result of greater heat circulation via Earth's oceans creating a smaller pole-to-tropic thermal gradient, changes in the land-sea geography driven by tectonism, and increased regional volcanism (Huber et al., 1995; Herman and Spicer, 2010).

Understanding Earth's climatic record is increasingly important for modeling and predicting the effects of modern climate change. Stable isotope geochemistry has become a common method for reconstructing Earth's climatic history. However, accurate geochemical profiles from bulk Cretaceous carbonate samples are difficult to assemble because post-depositional indicators often overprint original geochemical signals (Huber et al., 1995; Jenkyns et al., 2004).

Limited studies have been conducted on Slope Mountain strata and no stable isotope data currently exists local to our field site. However, a number of analogous studies of Middle-Cretaceous marine carbonates and sideritized carbonates do exist (McKay et al. 1995; Ufnar et al., 2008; Suarez et al. 2015). These studies investigate concretions and nodules, Middle-Cretaceous siderite-bearing paleosols, and Middle-Cretaceous bivalve fossils, respectively.

Our research uses geochemical and stable isotope analyses to compare data with prior Middle-Cretaceous climate studies. We assess whether the bulk stable isotope data from marine carbonate concretion and nodule samples are accurate stable isotope proxies

for climate. By comparing our data to prior regional studies, we hope to further the scientific understanding of Middle-Cretaceous climate.

Geologic Background

Tectonic Setting:

North Slope, Alaska (henceforth referred to as the North Slope) is a foreland basin that formed on the Arctic Alaska microplate (Figure 2).

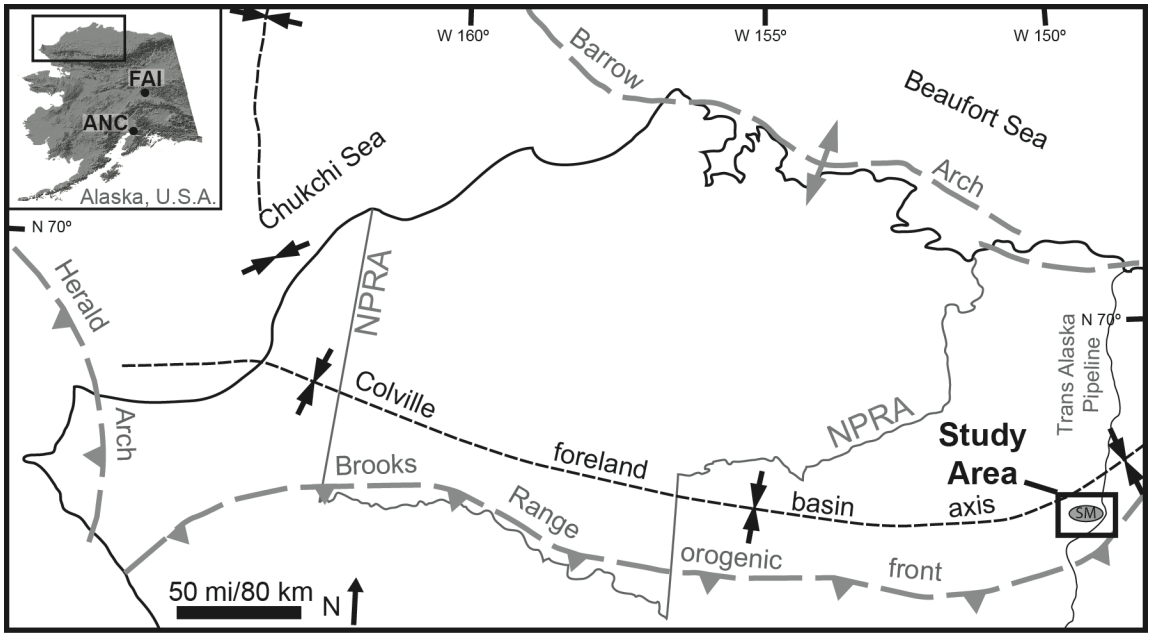

Figure 2: Regional map of the Colville Foreland Basin, North Slope, Alaska. Slope Mountain is located in the southeast quadrant of the figure and is denoted by "SM." Slope Mountain is located in the foothills of the Brooks Range, north of the Brooks Range orogenic front. The Colville Basin is bounded to the north by the Barrow Arch. Slope Mountain is made up of Brookian Sequence sediments that were deposited northward and eastward during the Brooks Range orogeny. Figure adapted from Bird and Molenaar, 1992, by Grant T. Shimer, Whitman College, and Paul J. McCarthy, University of Alaska Fairbanks.

The Arctic Alaska microplate developed along a passive continental margin and was likely an original piece of the North American continent (Bird and Molenaar, 1992). During the Jurassic and Cretaceous, rifting occurred along this passive margin and created the separate, present-day Arctic Alaska microplate. Rifting and counter-clockwise

rotation of the Arctic Alaska microplate away from the North American plate created the offshore Canada Basin and Beaufort passive margin (Bird and Molenaar, 1992).

Concurrent with rifting, on the opposite side of the Arctic Alaska microplate, a collision with an island arc system created the Brooks Range orogeny and Colville basin (Bird and Molenaar, 1992). The onshore portion of the basin is known as the Colville Basin and is bounded to the north by the Barrow Arch (LePain et al., 2009). The Barrow Arch is a structural and subsurface high that represents a rift shoulder that formed when the Arctic Alaska microplate separated from a northern landmass (LePain et al., 2009).

The tectono-stratigraphy of the North Slope can be divided into four unique sequences: the Franklinian Sequence, the Ellesmerian Sequence, the Beaufortian Sequence, and the Brookian Sequence. The bottommost unit is the Franklinian Sequence, which is a basement of pre-Mississippian varying lithologies and ages (Bird, 2001). The Ellesmerian Sequence refers to Upper Mississippian to Jurassic age sediments deposited from the north in a passive margin setting (Bird and Molenaar, 1992). The Beaufortian Sequence is a Jurassic to Lower Cretaceous mud-dominated succession of marine strata and local sandstones deposited during a period of active rifting (Bird, 2001). Lastly, the Brookian Sequence is made up of Lower Cretaceous to Pliocene age marine and nonmarine sediments shed northward and eastward from the Brooks Range orogenic belt (Bird, 2001). Slope Mountain is an exposure of marine, deltaic, and nonmarine sediments that forms part of the Brookian Sequence (Figure 3). Today, Slope Mountain is located directly west of both the Dalton Highway and the Trans-Alaska Pipeline System.

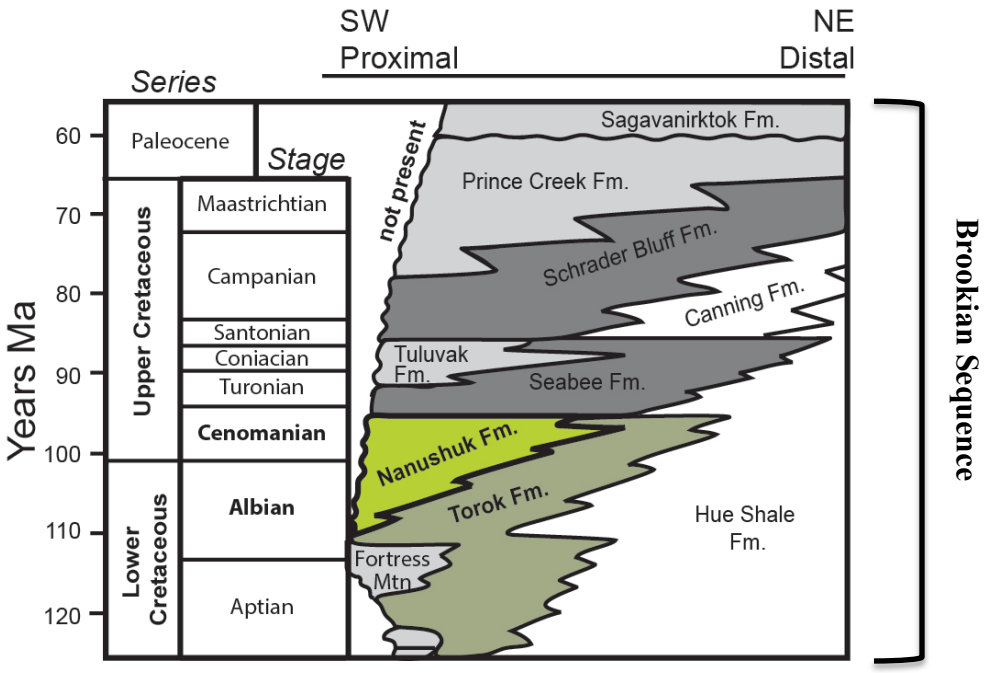

Figure 3: Central North Slope, Alaska, chronostratigraphic column. The units that this study investigates, the Torok Formation and Nanushuk Formation, are highlighted in green. Figure adapted from Mull et al., 2003, by Grant T. Shimer, Whitman College, and Paul J. McCarthy, University of Alaska Fairbanks.

Stratigraphy and Sedimentology:

During and prior to the early formation of the Canada Basin, passive margin activity from the north deposited Upper-Mississippian to Jurassic age sediments that are known as the Ellesmerian Sequence (Bird and Molenaar, 1992). Barrow Arch uplift during the Hauterivian led to widespread subaerial exposure and erosion of Neocomian and lower strata, creating the widespread Lower Cretaceous Unconformity (LCU) (Decker, 2007). In the area surrounding Slope Mountain, widespread uplift and exhumation in the Brooks Range between 135 Ma and 95 Ma resulted in sediment deposition in the Colville Basin from the south (LePain et al., 2009). The Nanushuk Formation, however, crops out across nearly the entire North Slope and much of the regional sediment was deposited in an east-northeast direction, prograding from the west. These sediments include deep water through nonmarine deposits of the Fortress

Mountain Formation, Torok marine shelf mudstones, and fluvial-deltaic-shelf strata of the Nanushuk Formation, respectively (LePain et al., 2009).

Together, the Nanushuk and upper Torok formations represent the change from an under-filled Colville Basin to an overfilled Colville Basin (LePain et al., 2009). The two units are exposed at the surface and subsurface throughout the foothills of the Brooks Range. The change in Colville Basin filling is attributed to the influx of sediment that was caused by uplift in the ancestral Brooks Range. Colville Basin filling peaked in the Albian, when the Nanushuk Formation overtopped the Barrow Arch (LePain et al., 2009).

The Torok Formation is recognized by mudstone facies deposited in marine slope and basin floor settings, and sandstone facies deposited in lower slope basin-floor turbidite settings (Mull et al., 2003). In the Slope Mountain area, the Torok Formation is exposed as shallow water mudstones (Johnsson and Sokol, 1998). The Nanushuk Formation is a succession of complexly intertonguing marine and nonmarine rocks deposited in fluvial, delta-plain, delta-front, prodelta, and shallow marine-shelf environments (Mull et al. 2003; LePain et al. 2009). In practice, it is common to distinguish between the marine Nanushuk Formation units, referred to as the lower Nanushuk Formation, and the marginal marine and terrestrial Nanushuk Formation units, referred to as the upper Nanushuk Formation. Gryc et al. (1951) originally identified and named the Nanushuk Group. The Nanushuk Formation was previously referred to as the Nanushuk Group and consisted of the following units (in descending order): Ninuluk Formation (marine), Niakogon and Killik Tongues of the Chandler Formation (nonmarine), Grandstand Formation (transitional marine and nonmarine), and Tuktu Formation (marine) (Mull et al., 2003). On the western North Slope, the former

Nanushuk Group consisted of, in descending order, the Corwin Formation (nonmarine) and the Kukpowruk Formation (marine). Mull et al. (2003) revise the stratigraphic nomenclature of the Nanushuk Group to comply with international stratigraphic guidelines. Mull et al. (2003) argues that a number of the distinct units lack the necessary credentials in order to be unique formations, i.e. are not able to be mapped in the field. Thus, they revised the nomenclature to upper Nanushuk Formation and lower Nanushuk Formation.

Carbonate nodules and concretions have been found throughout the Nanushuk Formation and Torok Formation (LePain et al., 2009). Concretions are diagenetic sedimentary structures that form when water is expelled out of sediment during compaction. As the sediment compacts, precipitate minerals fill the voids left by water and form a solid mass within the sediment. Recent studies suggest that siderite concretions and nodules are a valuable proxy for depositional environments, atmospheric heat transport, and paleohydrology (McKay et al., 1995; Ufnar et al., 2008).

Climate:

The climate of the Middle-Cretaceous is interpreted as an extremely warm greenhouse-world (Frakes, 1999; Wilson and Norris, 2001; Jenkyns et al. 2004; Huber et al., 2016). Wilson and Norris (2001) describe the Middle-Cretaceous as a period of anomalously warm high-latitude temperatures, reef drowning events at low-latitudes, and Oceanic Anoxic Events (OAEs). These events were likely the result of a smaller pole-to-tropic thermal gradient compared to that of today, increased atmospheric carbon dioxide (CO_2), and changes a different land-sea distribution than that of today (Huber et al., 2016).

The Cretaceous climate was not entirely stable throughout, as there were multiple warming and cooling events from the Early Cretaceous to the Late Cretaceous (Stoll and Schrag, 2000). Frakes (1999) explains that the Early Cretaceous was a time of relatively cooler sea-surface temperatures ranging from 0°C to 8°C from 126 Ma to 106 Ma. Warming, however, began during the Albian-Cenomanian and peaked at the Cenomanian-Turonian boundary at 90 Ma (Jenkyns et al., 2004). Peak temperatures during the Middle-Late Cretaceous surpassed 20°C and were as great as during any other period in Earth's history (Frakes 1999; Jenkyns et al. 2004).

Climatic conditions during the Cretaceous impacted atmosphere and ocean chemistry. Accurate geochemical profiles from bulk Cretaceous carbonate samples have proven difficult to compile because post-depositional artifacts often alter depositional geochemical signals (Jenkyns et al., 2004; Huber et al., 2016). The high-energy deltaic depositional environment of Nanushuk sediments also caused carbon contamination in marine settings. Wilson and Norris (2001), however, recorded $\delta^{18}O$ values ranging from 2 to -4‰. These values correspond to sea-surface temperatures ranging from 24°C to 32°C. As for $\delta^{13}C$, Gröcke et al. (2006), performed similar bulk sediment analyses that resulted in $\delta^{13}C$ values ranging from -23 to -26‰. A related study done by Jenkyns et al. (2004) found an average of temperature values of 15°C. One of the major intentions of the present research is to build upon prior Middle-Cretaceous isotope studies in order to improve the time period's geochemical profile.

$\delta^{13}C$ and $\delta^{18}O$ Stable Isotopes:

Isotopes are atoms of the same element with different numbers of neutrons. The differences in each atom's neutron number results in differences in molecular weight.

Isotopes can be classified by two distinctions: radioactive or stable. Stable isotopes do not decay over time. Oxygen has three naturally occurring stable isotopes: ^{16}O, ^{17}O, and ^{18}O. Carbon has two known stable isotopes: ^{12}C and ^{13}C. The greater the number of neutrons an atom has, the heavier the atom is.

Stable isotopes are most commonly referred to as the ratio of heavy isotopes to light isotopes compared to a standard ratio. The equation is as follows:

$$\delta = \left(\frac{R_S}{R_i - 1}\right) * 1000 \qquad \text{(Equation 1) (Kendall and McDonnell, 1998)}$$

Where δ refers to the resulting data, R_s refers to the heavy/light ratio of the sample, and where R_i refers to the heavy/light ratio of the standard. Samples returning positive values are referred to as heavy or enriched, and samples returning negative values are referred to as light or depleted.

Comparing experimental samples to standards is critical in order to accurately assess paleoclimates. For oxygen isotopes, the most common standard is the Vienna Standard Mean Ocean Water (VSMOW). VSMOW for $^{18}O/^{16}O$ is $2.0052 \cdot 10^{-3}$ (Kendall and McDonnell, 1998). For carbon isotopes, the most common standard is the Vienna Pee Dee Belemnite (VPDB), where VPDB for $^{13}C/^{12}C$ is $1.1237 \cdot 10^{-2}$ (Kendall and McDonnell, 1998).

The driving force behind $^{13}C/^{12}C$ ratios is the carbon cycle. The movement of organic and inorganic carbon between reservoirs such as the atmosphere, oceans, biomass, and sediment cause greater or lesser isotopic ratios of carbon to be reflected in the geologic record (Stanley, 1999). $\delta^{13}C$, therefore, has been used to extrapolate carbon

burial rates and weathering rates (Stanley, 1999). Gröcke et al. (2006), performed similar bulk carbonate analyses to our research that resulted in $\delta^{13}C$ values ranging from 23 to -26‰.

$\delta^{18}O$, on the other hand, varies with temperature, precipitation, and salinity (Stanley, 1999). The skeletons of marine fossils provide insight into paleoclimates' ocean temperatures. Mollusk- and snail-like organisms build their exteriors out of calcium carbonate ($CaCO_3$). In warm waters, organisms incorporate more ^{16}O relative to ^{18}O than in cooler waters (Stanley, 1999). Therefore, the warm periods of the Cretaceous should be reflected in relatively light $\delta^{18}O$ values compared to those of cooler times. Furthermore, ^{16}O evaporates more readily than ^{18}O and will refreeze in glaciers during cold periods (Stanley, 1999). Cold climates harbor relatively light $\delta^{18}O$ until they melt and flood the oceans with light oxygen (Stanley, 1999). Again, this would be reflected in the geologic record as periods of light $\delta^{18}O$ ratios. Wilson and Norris (2001), recorded Middle-Cretaceous $\delta^{18}O$ values ranging from -2 to-4‰. These values correspond to sea-surface temperatures ranging from 24°C to 32°C.

Methods

Field Surveying and Measured Sections:

The initial motivation for the field component of our research was to generate detailed stratigraphic sections of Slope Mountain, North Slope, Alaska (N68.75º W149.03º). Our field research team was comprised of six undergraduate geology students, two geology professors, and two paleontologists. Daily, the group of six geology students and one of the geology professors used Brunton compasses, Jacob's

staffs, hand-lenses, and grain-size cards to collect data and observations for what ultimately became eight unique stratigraphic sections. A handheld Garmin device was used to incrementally record GPS data for each section. For each stratigraphic section, lithology, strike and dip, and grain size were recorded in field notebooks. Measurements were most often made at meter-scale resolution, but finer-scale measurements were also made if we observed changes in grain size or bedding and if we observed sedimentary structures such as concretions and nodules, plant fossils, or ripple marks. In addition, comments on the locations of concretions and nodules, bivalve and gastropod fossils, leaf fossils, other plant fossils, carbonaceous organic matter, and *Rosselia socialis* fossils were noted when warranted. Figure 4 indicates the location of each of the eight measured stratigraphic sections. In regards to stratigraphic position, SM2 is the bottommost section and SM8 is the uppermost unit.

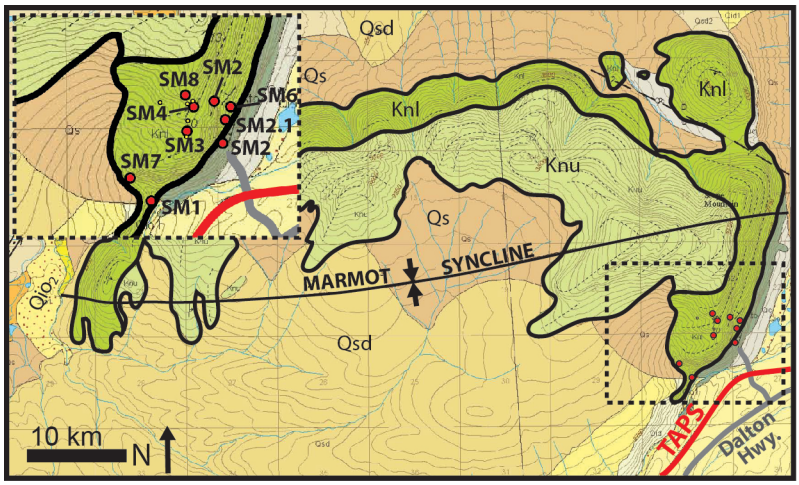

Figure 4: Geologic map of Slope Mountain, North Slope, Alaska, also known as the Marmot Syncline. The red dots indicate the location of our study site and measured stratigraphic sections. Our field site is located at the intersection between previously geologically mapped Torok Formation and Nanushuk Formation Units. We interpret our field site as Upper Torok Formation. Figure adapted from www.keckgeology.org by Grant T. Shimer, Whitman College, and Paul j. McCarthy, University of Alaska Fairbanks.

Areas covered by talus slope were measured to the best of our team's abilities, but due to time constraints, we made the assumption of homogenous lithology and grain size for

covered portions of SM2. These sections of SM2 were predominately fine-grained mudstones. We drafted and finalized measured stratigraphic sections at the Geology Departments of the University of Alaska Fairbanks and Whitman College.

Concretion and Nodule Sampling:

In addition to measuring the stratigraphy at Slope Mountain, my research objective extended to collecting concretions and nodules for geochemical analyses. Carbonates reported as "nodules" were considered concretions because a clear distinction could not be made (Figure 5).

Figure 5: Sample photos of SM2-JB-4m. This serves as an example for concretions and nodules that were observed in the field. SM2-JB-4m, in-situ, surrounded by mudstone layers (left) and SM2-JB-4m, post-collection, in the University of Alaska Geology Department laboratory. All field samples were collected as wholly as possible and then cut using the University of Alaska Geology Department's rock-saw.

Thirty total samples were collected from the eight stratigraphic sections on Slope Mountain. The 30 samples were identified as concretions or nodules in the field, but would later be investigated more deliberately. All 30 concretion and nodule samples were

collected in-place with a rock-hammer. The size of the 30 samples ranged from 3 to 12cm in diameter.

In addition to the 30 in-place samples, four bulk float samples were collected. The float samples are of unknown origin, but they were collected for comparison with the 30 in-place samples. The float samples were comprised of what we defined as possibly sideritized carbonate clasts and shards.

Samples were cut using the University of Alaska Fairbanks' Geosciences department's rock-saw, and Spectrum Petrographics prepared thin sections for later mineralogical analyses at Washington and Lee University. Hydrochloric acid (10%) was initially used to determine the presence of carbonate minerals. Both the in-place and float samples were powdered using a mortar and pestle or Washington and Lee University's SPEX SamplePrep 8510 Shatterbox for x-ray diffraction and isotopic analysis. Bulk samples were used for all x-ray diffraction and isotope analyses.

X-Ray Diffraction Analyses:

X-ray diffraction analyses were conducted using Washington and Lee University's Diano 2100 E X-ray diffractometer. A sufficient amount of each sample's powder was mounted to a 1" x 2" glass slide using 99% isopropyl alcohol. Each sample rate scan time lasted 20 minutes. One sample was run for 7 hours in order to assess the relationship between scan time and result quality. From the identified and assumed mineralogy, 2-Theta Rates were assessed between 20° and 80°. The x-ray diffraction machine used Cu radiation and was set to 40 Kv. Many of the in-place and float samples were hypothesized to contain siderite minerals. Furthermore, a layer of SM2 was

considered to be a possible tephra layer. The x-ray diffraction results were used to more accurately assess the mineralogy of each sample.

$\delta^{13}C$ and $\delta^{18}O$ Analyses:

Additional sample powder was created using the aforementioned Shatterbox and analyzed for $\delta^{13}C$ and $\delta^{18}O$ ratios using Washington and Lee University's Thermo Scientific Delta V Advantage mass spectrometer and Finnigan GasBench II. Powdered samples were weighed to an average of 500 µg using Washington and Lee University's Sartorius Cubis Series MSE-3.6p mass balance. Many of the samples were classified as "dirty carbonates," distinguishing them from pure carbonate samples solely composed of $CaCO_3$. Triplets of each sample were run to assess sample heterogeneity. After weighing each sample, the powders were flushed with 99% compressed He and then pressurized to remove any present-day atmospheric $\delta^{13}C$ or $\delta^{18}O$ signatures. Pure crystalized Acros Organics phosphoric acid was melted into a liquid on a hot plate. This liquefied phosphoric acid was next reacted with each pressurized sample for no less than two hours. The prepared samples were then run in the mass spectrometer. $\delta^{13}C$ and $\delta^{18}O$ data were compared to the NIST NBS19 standard. $\delta^{13}C$ sample data were then corrected with reference to the Pee Dee Belemnite (PDB) standard, while $\delta^{18}O$ were corrected with reference to the Vienna Standard Mean Ocean Water (VSMOW) using the equation from Sharp (2007):

$$\delta^{18}\text{O VSMOW} = 1.03086 * (\delta^{18}\text{O VPDB}) + 30.86 \text{ (Equation 2)}$$

Data were only used for samples that returned a standard deviation less than 0.1 and contained significant amounts of $CaCO_3$, determined by a return of at least eight XRD peaks. The mass spectrometer data were analyzed using Isodat Acquisition software and then transferred to Microsoft Excel for plotting. $\delta^{13}C$ and $\delta^{18}O$ were plotted against each other and $\delta^{13}C$ and $\delta^{18}O$ were then individually plotted stratigraphically.

Results

XRD Analyses:

The purpose of our XRD analyses was to better determine concretion and nodule mineralogy. LePain et al. (2009) describes many of these concretions and nodules as containing siderite. The results of our XRD scans, however, do not suggest a significant siderite presence. Furthermore, five of our XRD scans did not return any identifiable peaks. In order to correct for this issue, we increased the XRD rate scan time and let one sample run overnight. This technique did not have a significant effect on our results. Figure 6 displays the results of our XRD analyses. With the exception of quartz and carbonate, no additional mineralogy was able to be confidentially determined (Figure 6).

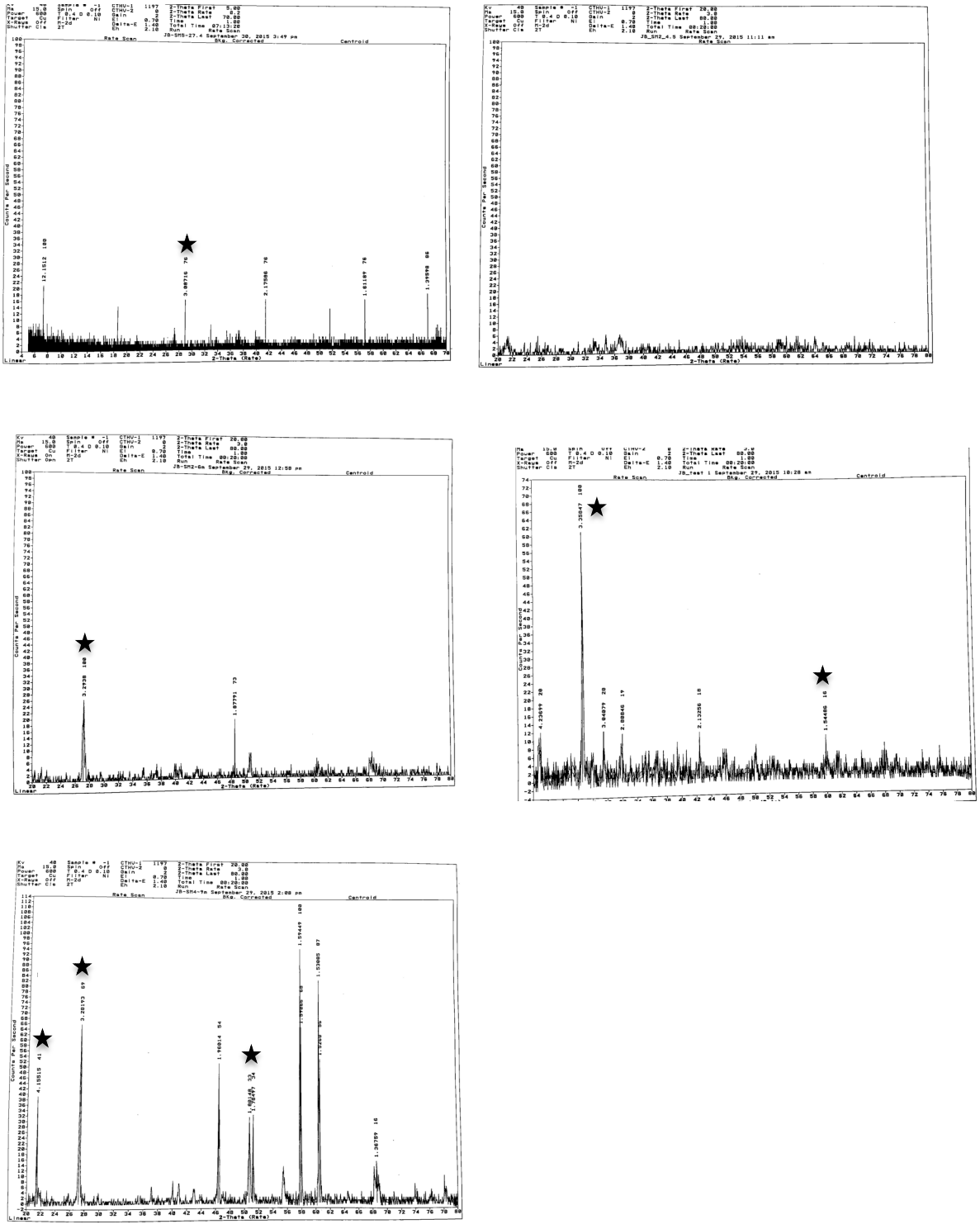

Figure 6: XRD scans for concretion and nodule samples: SM5-JB-27.4m, SM2-JB-4.5m, SM2-JB-6m, SM2-JB-39.5m, and SM2-JB-9m (starting top-left and reading accordingly). With the exception of SM5-JB-27.4m, each image represents a 20-minute XRD scan. The top left sample was run overnight for seven hours. The XRD machine used Cu kα radiation set to 40 Kv. No significant siderite presence is detected and, due to the lack of identifiable peaks, no mineralogy except for quartz was confidentially determined. ★ represent quartz peaks.

Stable Isotope Analyses:

$\delta^{18}O$ results range from 17.40 to 28.10‰ with an average value of 23.66‰. $\delta^{13}C$ results range from -21.73 to 2.20‰ with an average value of -6.19‰ (Table 1). $\delta^{18}O$ and $\delta^{13}C$ were compared to three different studies: McKay et al. (1995), Ufnar et al. (2008), and Suarez et al. (2015). Figure 7 is a plot of data from this study plotted against data from these prior studies. With the exception of one sample from McKay et al. (1995), our results comprise the range of all of these studies' data. Our data can be seen as bounding in a both the positive and negative direction to the proxy studies' data. In our study, $\delta^{13}C$ returned greater variation than $\delta^{18}O$, with a standard deviation of 8.38‰. Our $\delta^{18}O$ results show lesser variation, with a standard deviation of 2.52‰. Our $\delta^{18}O$ and $\delta^{13}C$ results produce a small positive slope of 0.16. Data from McKay et al. (1995) and Suarez et al. (2015) also reflect similar positive linear slopes between $\delta^{18}O$ and $\delta^{13}C$.

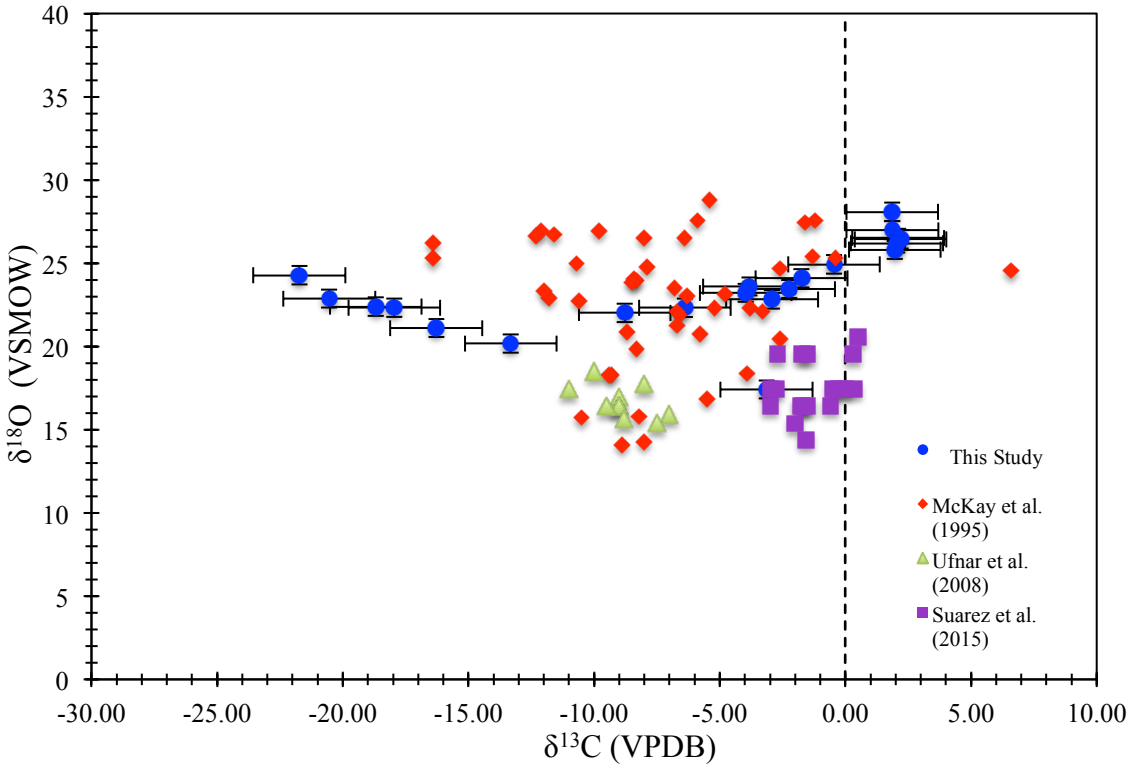

Figure 7: Plot showing $\delta^{18}O$ plotted against $\delta^{13}C$. Data from McKay et al. (1995), Ufnar et al. (2008), and Suarez et al. (2015) are included. Data from this study encompass and serve as boundaries for the supplemental data. A gentle positive and linear slope exists between $\delta^{18}O$ and $\delta^{13}C$ for this study's data. $\delta^{13}C$ values have greater variance than $\delta^{18}O$ values. The error bars on this study's data depict standard error.

Figure 8 shows our $\delta^{18}O$ and $\delta^{13}C$ data plotted against their respective stratigraphic positions on Slope Mountain. Again, $\delta^{13}C$ data show greater variance than $\delta^{18}O$ data. $\delta^{13}C$ values, on the other hand, vary with geologic time and Cretaceous climate change. $\delta^{13}C$ tend to be more enriched moving up Slope Mountain, with two positive $\delta^{13}C$ excursions at 35.7 m and 45 m (Figure 8).

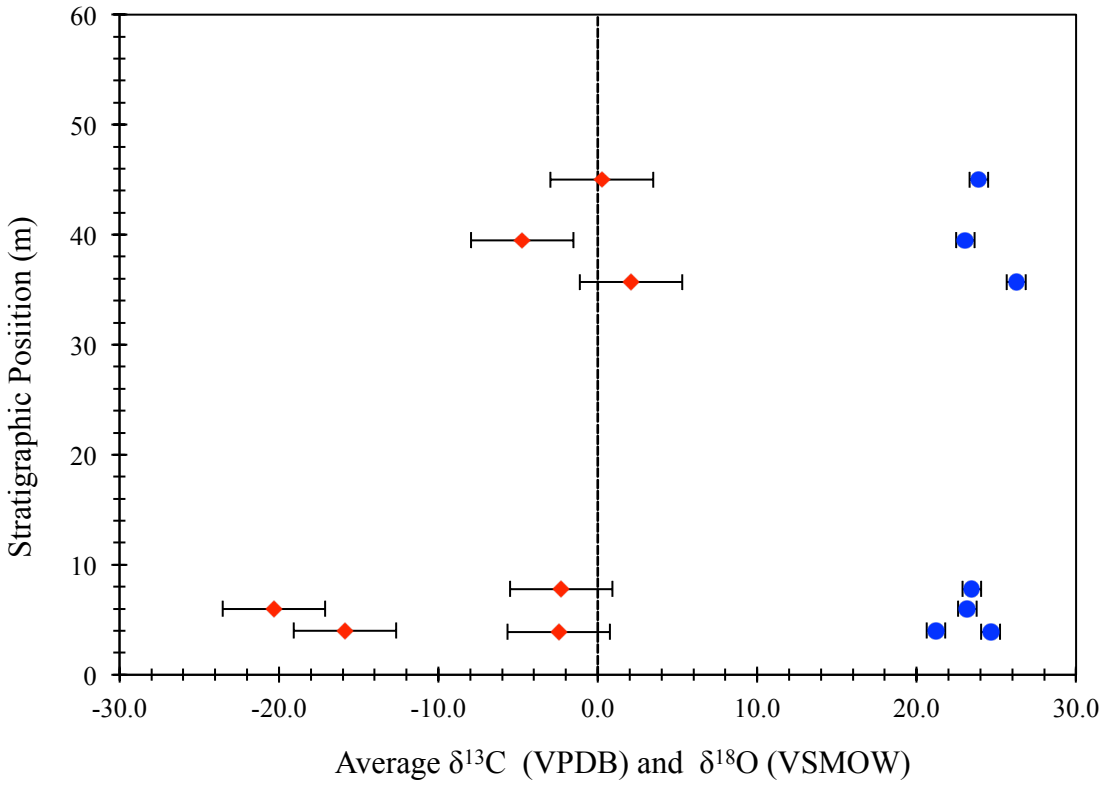

Figure 8: Average δ^{18}O and δ^{13}C each plotted against their stratigraphic position on Slope Mountain. These data are derived from the average values of each sample's triplet. Notice the consistent δ^{18}O ‰ VSMOW values contrasted against more variable δ^{13}C‰ VPDB values that become more enriched moving up Slope Mountain. Error bars depict standard error.

Table 1: Tabular representation of all concretion and nodule $\delta^{18}O$ and $\delta^{13}C$ data. For each sample at a unique stratigraphic location, triplet bulk powder samples were run for $\delta^{18}O$ and $\delta^{13}C$ ratios. Average values for this triplet procedure are included. Below, fundamental statistics show comprehensive mean, maximum, minimum, and standard deviation values.

Sample	Stratigraphic Position (m)	Average δ18O (VSMOW)	δ18O (VSMOW)	Average δ13C (VPDB)	δ13C (VPDB)
SM2-JB-3.9M-A	3.90		27.00		1.87
SM2-JB-3.9M-B	3.90		22.00		-8.78
SM2-JB-3.9M-C	3.90	24.60	24.90	-2.50	-0.45
SM2-JB-4M-A	4.00		21.10		-16.28
SM2-JB-4M-B	4.00		20.20		-13.32
SM2-JB-4M-C	4.00	21.20	22.30	-15.90	-17.95
SM2-6MCON-A	6.00		22.40		-18.69
SM2-JB-6MCON-B	6.00		22.90		-20.54
SM2-JB-6MCON-C	6.00	23.20	24.30	-20.30	-21.73
SM2-JB-7.8M-A	7.80		24.10		-1.74
SM2-JB-7.8M-B	7.80		22.80		-2.92
SM2-JB-7.8M-C	7.80	23.50	23.40	-2.30	-2.24
SM1-JB-7.2M-A	35.70		25.80		1.97
SM1-JB-7.2M-B	35.70		26.50		2.10
SM1-JB-7.2M-C	35.70	26.30	26.40	2.10	2.20
SM2-JB-39.5M-A	39.50		23.60		-3.82
SM2-JB-39.5M-B	39.50		22.30		-6.39
SM2-JB-39.5M-C	39.50	23.00	23.20	-4.70	-3.97
SM2-JB-45M-A	45.00		26.20		2.06
SM2-JB-45M-B	45.00		17.40		-3.13
SM2-JB-45M-C	45.00	23.90	28.10	0.30	1.86
	Mean:		23.66		-6.19
	Max:		28.10		2.20
	Min:		17.40		-21.73
	Standard Deviation:		2.52		8.38

Discussion

Our study attempts to use $\delta^{18}O$ and $\delta^{13}C$ data from marine carbonate concretions and nodules as a proxy to refine the understanding of Middle-Cretaceous climate conditions. We use XRD analyses to assess the mineralogy of these marine carbonate concretions and nodules, as well as stable isotope analyses to extrapolate temperature conditions ($\delta^{18}O$) and carbon cycle dynamics ($\delta^{13}C$).

We use depositional environment and sedimentary structure analogues for which to compare our $\delta^{18}O$ and $\delta^{13}C$ data to those of prior studies: our samples are all taken from marine environments, and our samples are all concretions or nodules. Suarez et al. (2015) investigated stable isotope data from Middle-Cretaceous bivalve shells to interpret climate, but not data from concretions. Ufnar et al. (2008) used stable isotope data from Middle-Cretaceous siderite bearing paleosols for paleoclimate analyses, and while these samples may have similar mineralogy, they are from different depositional environments. Nonetheless, both datasets show paleohydrology and atmospheric heat transport evidence for a greenhouse Middle-Cretaceous. Our results present an interesting intersection between both previous studies; our marine carbonate concretions and nodules incorporate the marine aspect of Suarez et al. (2015) and the supposedly Middle-Cretaceous siderite aspect of Ufnar et al. (2008). Furthermore, Mozley and Burns (1993) conducted a global study on concretionary marine carbonate samples and recorded values for $\delta^{13}C$ ranging from -40 to 10‰ and values for $\delta^{18}O$ ranging from 14 to 30‰. A study done by Wilson and Norris (2001) on Middle-Cretaceous foraminifera produced $\delta^{18}O$ values ranging from 27 to 29‰. These values correspond to sea-surface temperatures ranging from 24 to 32°C

and lie in accordance with our data. Their study, however, reports $\delta^{13}C$ values between 0 to 3‰, which align with the minority of our data.

Johnsson and Sokol (1998) is the only stratigraphic field study that has focused extensively on Slope Mountain. Their interpretation of the area as a high-energy, prograding deltaic system supports the possibility of terrestrial matter being introduced into marine environments. We attribute the large $\delta^{13}C$ variance in our data to terrestrial variable contamination of plant and woody matter. The introduction of terrestrial $\delta^{13}C$ into our system would result in both meteoric and ocean influenced data. Our $\delta^{18}O$ results agree with these data, and while our $\delta^{13}C$ also fall within this range, the $\delta^{13}C$ data variance is too large to significantly draw conclusions relating to carbon-cycle dynamics.

Stratigraphic position does not reflect any significant trends in $\delta^{18}O$ values, as the data remain vertically consistent. The consistency of our $\delta^{18}O$ data versus our $\delta^{13}C$ data warrants further investigation. The lack of variance between our $\delta^{18}O$ results suggests that the Middle-Cretaceous was a warm period throughout the deposition of our samples. The variance between our $\delta^{13}C$ results suggests that there may have been finer timescale changes to the depositional environments of Slope Mountain sediments. Johnsson and Sokol's (1998) high-energy delta interpretation would support this hypothesis, as this setting would result in terrestrial matter being fluxed into the marine system. This larger range of $\delta^{13}C$ results reflects terrestrial and marine carbon.

One of the major limitations of the present study is the undetermined concretion and nodule mineralogy. The concretions were initially believed to contain large amounts of siderite, but our XRD analyses did not prove this to be correct. Given the agreement of our $\delta^{18}O$ and $\delta^{13}C$ data to that of Ufnar et al. (2008), it is possible that the concretions

once contained significant percentages of siderite, but the minerals have been diagenetically altered and are now interpreted as amorphous.

Secondly, our concretions and nodules contained varying amounts of carbonate minerals. Some of our samples had to be run multiple times in the mass spectrometer in order to generate significant isotope data. Moving forward, total organic carbon (TOC) analyses would aid in better understanding our samples' composition. Lastly, radiometrically dating our samples may more precisely determine whether these samples are Aptian, Albian, or Cenomanian (all Middle-Cretaceous) in age. These interpretations and assumptions have significant implications for our $\delta^{18}O$ and $\delta^{13}C$ results because our data may reflect isotopic signals of intensely altered and amorphous minerals.

Conclusions

The results of our $\delta^{18}O$ stable isotope analyses are in agreement with prior studies that suggest a greenhouse Middle-Cretaceous climate. By comparing our data to that of prior studies, we were able to refine the understanding of Middle-Cretaceous climate and add isotope data local to Slope Mountain to the scientific community. Further analyses must be done to better understand the mineralogy and geochemistry surrounding the reported siderite concretions and nodules. With these analyses, concretion and nodule studies investigating paleoclimate will be much more reliable. Given the implications of our results, we suggest that further concretion and nodule research is done to understand paleoclimatic conditions.

Acknowledgements

I would like to thank the KECK Geology Consortium for funding and organizing this research opportunity. I would also like to thank Dr. Grant T. Shimer, Whitman College, and Dr. Paul J. McCarthy, University of Alaska Fairbanks, for their support throughout the field and laboratory aspects of my project. I thank Dr. Lisa Greer, Washington and Lee University, for advising me throughout the writing process, as well as Emily Falls, Washington and Lee University, for her constant technical and analytical support.

Works Cited

Bird, K.J., and Molenaar, C.M., 1992, The North Slope foreland basin, Alaska, *in* Macqueen, R.W., and Leckie, D.A., eds., Foreland fold & thrust belts: AAPG Memoir 55, p. 363–393.

Bird, K. J., 2001, Alaska: A twenty-first-century petroleum province, *in* M.W. Downey, J. C. Threet, and W. A. Morgan, eds., Petroleum provinces of the twenty-first century: AAPG Memoir 74, p. 137–165

Decker, P. L. "Brookian Sequence Stratigraphic Correlations, Umiat Field to Milne Point Field, West-central North Slope, Alaska." (2007): n. pag. Web.

Frakes, Larry A. "Estimating the global thermal state from Cretaceous sea surface and continental temperature data." *Special Papers-Geological Society of America* (1999): 49-58.

Gröcke, Darren R., et al. "Recognizing the Albian-Cenomanian (OAE1d) sequence boundary using plant carbon isotopes: Dakota Formation, Western Interior Basin, USA." *Geology* 34.3 (2006): 193-196.

Gryc, George, Patton, W.W., Jr., and Payne, T.G., 1951, Present Cretaceous stratigraphic nomenclature of northern Alaska: Washington Academy of Sciences Journal, v. 41, no. 5, p. 159–167.

Herman, Alexei B., and Robert A. Spicer. "Mid-Cretaceous floras and climate of the Russian high Arctic (Novosibirsk Islands, northern Yakutiya)." *Palaeogeography, Palaeoclimatology, Palaeoecology* 295.3 (2010): 409-422.

Huber, Brian T., David A. Hodell, and Christopher P. Hamilton. "Middle–Late Cretaceous climate of the southern high latitudes: stable isotopic evidence for minimal equator-to-pole thermal gradients." *Geological Society of America Bulletin* 107.10 (1995): 1164-1191.

Jenkyns, Hugh C., et al. "High temperatures in the late Cretaceous Arctic Ocean." *Nature* 432.7019 (2004): 888-892.

Johnsson, M.J., and Sokol, N.K., 2000, Stratigraphic variation in petrographic composition of Nanushuk Group sandstones at Slope Mountain, North Slope, Alaska, in Kelley, K.D., and Gough, L.P., eds., Geologic studies in Alaska by the U. S. Geological Survey, 1998: U.S. Geological Survey Professional Paper 1615, p. 83-100.

Kendall, Carol, and Eric A. Caldwell. "Fundamentals of isotope geochemistry." *Isotope tracers in catchment hydrology* (1998): 51-86.

LePain, David L., Paul J. McCarthy, and Russell Kirkham. "Sedimentology, Stacking Patterns, and Depositional Systems in the Middle Albian-Cenomonian Nanushuk Formation in Outcrop, Central North Slope, Alaska." *Http://dggs.alaska.gov*. State of Alaska Department of Natural Resources, 2009. Web. 5 Aug. 2015.

Marshall, J. D. and Pirrie, D. (2013), Carbonate concretions—explained. Geology Today, 29: 53–62. doi: 10.1111/gto.12002

McKay, J., Longstaffe, F., and Plint, A., 1995, Early diagenesis and its relationship to depositional environment and relative sea-level fluctuations (Upper Cretaceous Marshybank Formation, Alberta and British Columbia): *Sedimentology,* v. 42, p. 161-190, doi: 10.1111/j.1365-3091.1995.tb01276.x.

Mozley, Peter S., and Stephen J. Burns. "Oxygen and carbon isotopic composition of marine carbonate concretions: an overview." *Journal of Sedimentary Research* 63.1 (1993).

Mull, C.G., Houseknecht, D.W., and Bird, K.J., 2003, Revised Cretaceous and Tertiary stratigraphic nomenclature in the Colville Basin, northern Alaska: U.S. Geological Survey Professional Paper 1673, 51p.

NOAA National Centers for Environmental Information, State of the Climate: Global Analysis for Annual 2014, published online January 2015, retrieved on February 1, 2016 from http://www.ncdc.noaa.gov/sotc/global/201413.

Pirrie, D., et al. "Cool early Albian climates; new data from Argentina." *Cretaceous Research* 25.1 (2004): 27-33.

Reifenstuhl, R.R., and Plumb, E.W., 1993, Micropaleontology of 38 outcrop samples from the Chandler Lake, Demarcation Point, Mt. Michelson, Philip Smith Mountains, and Sagavanirktok quadrangles, northeast Alaska: Alaska Division of Geological & Geophysical Surveys Public Data File 93-30B, 15 p., 4 sheets, scale 1:250,000. doi:10.14509/1565

Sharp, Zachary. *Principles of stable isotope geochemistry*. Upper Saddle River, NJ: Pearson Education, 2007.

Stanley, Steven M. *Earth System History*. New York: W.H. Freeman, 1999. Print.

Stoll, Heather M., and Daniel P. Schrag. "High-resolution stable isotope records from the Upper Cretaceous rocks of Italy and Spain: Glacial episodes in a greenhouse planet?." *Geological Society of America Bulletin* 112.2 (2000): 308-319.

Suarez, C., Flaig, P., Ludvigson, G., González, L., Tian, R., Zhou, H., McCarthy, P., Van der Kolk, D., and Fiorillo, A., 2015, Reconstructing the paleohydrology of a cretaceous Alaskan paleopolar coastal plain from stable isotopes of bivalves:

Palaeogeography, Palaeoclimatology, Palaeoecology, v. 441, p. 339-351, doi:10.1016/j.palaeo.2015.07.025.

Tajika, Eiichi. "Carbon cycle and climate change during the Cretaceous inferred from a biogeochemical carbon cycle model." *Island Arc* 8.2 (1999): 293-303.

Ufnar, D., Ludvigson, G., González, L., and Gröcke, D., 2008, Precipitation rates and atmospheric heat transport during the Cenomanian greenhouse warming in North America: estimates from a stable isotope mass-balance model: *Palaeogeography, Palaeoclimatology, Palaeoecology*, v. 266, p. 28-38, doi: 10.1016/ j.palaeo.2008.03.033.

Wilson, Paul A., and Richard D. Norris. "Warm tropical ocean surface and global anoxia during the mid-Cretaceous period." *Nature* 412.6845 (2001): 425-429.